Ehlers–Danlos Syndrome Associated with Glycosaminoglycan Abnormalities

10

Noriko Miyake, Tomoki Kosho, and Naomichi Matsumoto

Abstract

Ehlers–Danlos syndrome (EDS) is a genetically and clinically heterogeneous group of connective tissue disorders that typically present with skin hyperextensibility, joint hypermobility, and tissue fragility. The major cause of EDS appears to be impaired biosynthesis and enzymatic modification of collagen. In this chapter, we discuss two types of EDS that are associated with proteoglycan abnormalities: the progeroid type of EDS and dermatan 4-*O*-sulfotransferase 1 (D4ST1)-deficient EDS. The progeroid type of EDS is caused by mutations in *B4GALT7* or *B3GALT6*, both of which encode key enzymes that initiate glycosaminoglycan (GAG) synthesis. D4ST1-deficient EDS is caused by mutations in *CHST14*, which encodes an enzyme responsible for post-translational modification of GAG. The clinical and molecular characteristics of both types of EDS are described in this chapter.

Keywords

Ehlers–Danlos syndrome (EDS) • Progeroid type • *B4GALT7* • *B3GALT6* • Xylosylprotein beta 1,4-galactosyltransferase, polypeptide 7 • UDP-Gal:βGal β 1,3-galactosyltransferase polypeptide 6 • Dermatan 4-*O*-sulfotransferase 1 (D4ST1)-deficient EDS • *CHST14*

N. Miyake (✉) • N. Matsumoto
Department of Human Genetics, Yokohama City University Graduate School of Medicine, 3-9 Fukuura, Kanazawa-ku, Yokohama, 236-0004, Japan
e-mail: nmiyake@yokohama-cu.ac.jp; naomat@yokohama-cu.ac.jp

T. Kosho
Department of Medical Genetics, Shinshu University School of Medicine, 3-1-1 Asahi, Matsumoto, 390-8621, Japan
e-mail: ktomoki@shinshu-u.ac.jp

J. Halper (ed.), *Progress in Heritable Soft Connective Tissue Diseases*, Advances in Experimental Medicine and Biology 802, DOI 10.1007/978-94-007-7893-1_10,

Abbreviations

CHST14	Carbohydrate (*N*-Acetylgalactosamine 4-*O*) Sulfotransferase 14
D4ST1	Dermatan 4-*O*-sulfotransferase 1
EDS	Ehlers–Danlos Syndrome
GAG	Glycosaminoglycan
Gal	Galactose
GalNAc	*N*-Acetylgalactosamine
GlcA	Glucuronic Acid
IdoA	Iduronic Acid
PG	Proteoglycan
Xyl	Xylose

10.1 Introduction

Ehlers–Danlos syndrome (EDS) is a heterogeneous connective tissue disorder that affects as many as 1 in 5,000 individuals. It is characterized by joint and skin laxity, and tissue fragility [44]. In a revised classification, Beighton et al. classified EDS into six major types and several minor types [2]. The major causes of EDS are thought to include abnormal collagen biosynthesis through dominant-negative effects, haploinsufficiency of mutant procollagen α-chains, or deficiencies in collagen processing enzymes [29]. Abnormal glycosaminoglycan (GAG) synthesis and incorrect post-translational modification of GAG in proteoglycans (PGs) were recently identified in the progeroid type of EDS (EDS, progeroid form; MIM#130070, MIM#615349) and dermatan 4-*O*-sulfotransferase 1 (D4ST1)-deficient EDS (EDS, musculocontractural type; MIM#601776), respectively. In this chapter, the clinical and molecular characteristics of both types of EDS are described.

10.2 Background

Glycosylation is the addition of a sugar chain (a glycan) to a protein (generating a glycoprotein) or lipid (generating a glycolipid). More than 40 human disorders are thought to be caused by abnormal glycosylation [15, 19]. PGs are composed of core proteins and one or more glycans with modifications. PGs are present in the extracellular matrix and have important diverse biological functions [5]. PG synthesis is initiated by the sequential addition of four monosaccharides (xylose [Xyl], two molecules of galactose [Gal] and glucuronic acid [GlcA]), known as a linker tetrasaccharide, to the serine residue of the core protein backbone (Fig. 10.1a). Additional sugar chains are extended from the linker tetrasaccharide by the addition of repeated disaccharides (usually consisting of 50–150 disaccharides in vivo). Afterwards, some sugars are modified by a series of epimerases (epimerization) and sulfotransferases (sulfation).

GAGs are long unbranched polysaccharides consisting of repeating disaccharide units. GAGs are highly negatively charged because of the acidic sugar residues and/or sulfation. Consequently, GAG can change its conformation, attract cations, and bind water. Hydrated GAG gels enable joints and tissues to absorb large pressure changes, providing tissue elasticity. Post-translational modifications such as epimerization, sulfation, and acetylation/deacetylation result in the formation of diverse motifs in the GAG chains, which can bind to a large variety of ligands. Therefore, GAG chains play important roles in regulating growth factor signaling, cell adhesion, proliferation, differentiation, and motility [3, 5, 45].

GAGs can be divided into two groups: (1) galactosaminoglycans such as chondroitin sulfate (CS) and dermatan sulfate (DS), and (2) glucosaminoglycans such as hyaluronic acid, keratan sulfate, heparan sulfate, and heparin [42]. Two types of glycosylation are known: *O*-glycosylation and *N*-glycosylation (Fig. 10.2a). Most GAGs (except for keratan sulfate and hyaluronic acid) are *O*-glycans that bind to the glycan via an oxygen molecule in the serine or threonine residue of the core protein (Fig. 10.2a). Notably, failure to add the first or second galactose residue of the tetrasaccharide results in the progeroid type of EDS (Fig. 10.1b, c).

The CS and DS GAGs are produced via the same pathway (Fig. 10.3a). In this pathway, after the linker tetrasaccharide attaches to the serine

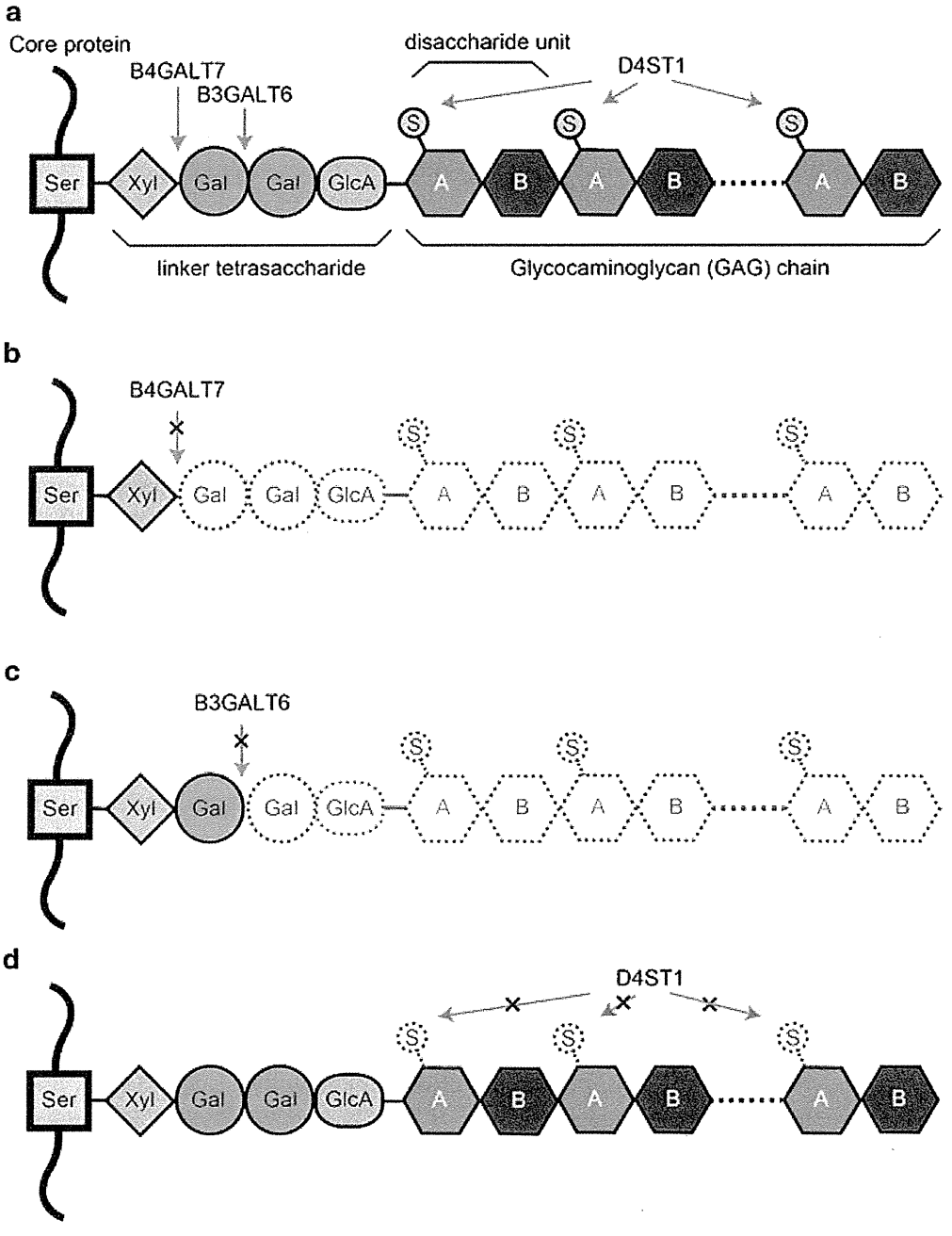

Fig. 10.1 Proteoglycan biosynthesis and its defects in two types of EDS. (**a**) Normal state. The serine residue (Ser) of the core protein and the GAG chain are bound via a linker tetrasaccharide. In CS, the disaccharides are composed of N-acetylgalactosamine (GalNAc) [position A] and glucuronic acid [position B]. In DS, the disaccharides are composed of GalNAc [position A] and Iduronic acid (IdoA) [position B]. B4GALT7 and B3GALT6 add the first and second galactose (Gal) to the xylose of the linker tetrasaccharide (*green arrows*). D4ST1 then adds the active sulfate to the 4-*O* position of GalNAc (*red arrows*) on DS. (**b**, **c**) Progeroid type of EDS. The impaired B4GALT7 cannot elongate the glycan chain from the first galactose (**b**). The impaired B3GALT6 cannot add the second galactose and the following glycan chain (**c**). (**d**) D4ST1-deficient EDS. The impaired/inactive D4ST1 cannot add the sulfate to GalNAc. *Gal* galactose, *GlcA* glucuronic acid, *S* active sulfate, *Ser* serine, *Xyl* xylose

residue of the core protein, GalNAc (*N*-acetyl galactosamine) transferase I elongates the glycan branch to create CS/DS. The enzyme C5-carboxy epimerase transforms glucuronic acid (GlcA) to iduronic acid (IdoA), which is specific for dermatan/DS (Fig. 10.3a). DS actually exists in a CS/DS hybrid state, containing GlcA–GalNAc and IdoA–GalNAc disaccharides (Figs. 10.2b

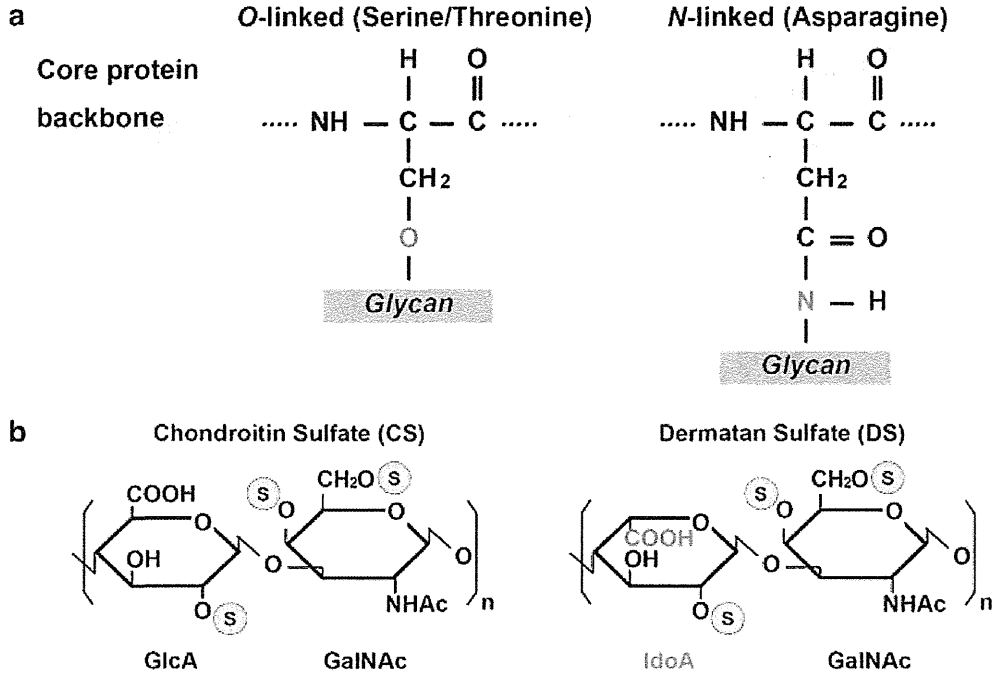

Fig. 10.2 Chemical structures of proteoglycan and disaccharides. (**a**) Chemical structure of *O*-linked and *N*-linked glycan. *O*-linked glycan can be linked via the *O*-element of serine or threonine. The diagram shows linking for serine. (**b**) Chemical structures of the disaccharide units of CS (*left*) and DS (*right*)

and 10.3a) [12]. Dermatan 4-*O*-sulfotransferase 1(D4ST1) specifically transfers an active sulfate to the 4-*O* position on the GalNAc residue of dermatan. The transfer of the active sulfate is impaired in D4ST1-deficient EDS (Figs. 10.1d and 10.3b).

10.3 The Progeroid Type of EDS (type 1: MIM#130070, type2: MIM#615349)

Alternative Names (MIM#130070)
Xylosylprotein 4-β-galactosyltransferase deficiency
XGPT deficiency
Galactosyltransferase I deficiency

10.3.1 Clinical Manifestations

Hernandez et al. reported five unrelated males in 1979, 1981, and 1986 representing a distinct variant of EDS. These males presented with a progeroid facial appearance, mild intellectual disability, and multiple nevi, in addition to hyperextensibility and fragility of skin, a high propensity for bruising, and joint hypermobility (particularly of the digits) [16–18]. A wrinkled face, curly and fine hair, scant eyebrows/eyelashes, telecanthus, periodontitis, multiple caries, low set/prominent ears, pectus excavatum, winged scapulae, and pes planus were observed in all five patients. Cryptorchidism and inguinal hernia were also noticed in four of the patients. Interestingly, the occurrence of the disorder in all of these patients was sporadic and the ages of their fathers were relatively advanced (33–55 years old). These characteristics prompted Hernandez et al. to speculate that the syndrome is caused by a de novo mutation [16].

In 1987, Kresse et al. reported a Danish male patient who was born to non-consanguineous healthy parents [26]. This patient presented with the clinical features observed in the original five patients, as well as a triangular head with a tiny face, frontal bossing, mid-face hypoplasia, a broad nasal bridge, prominent deep-set eyes, a small mouth, dental anomalies, low-set ears,

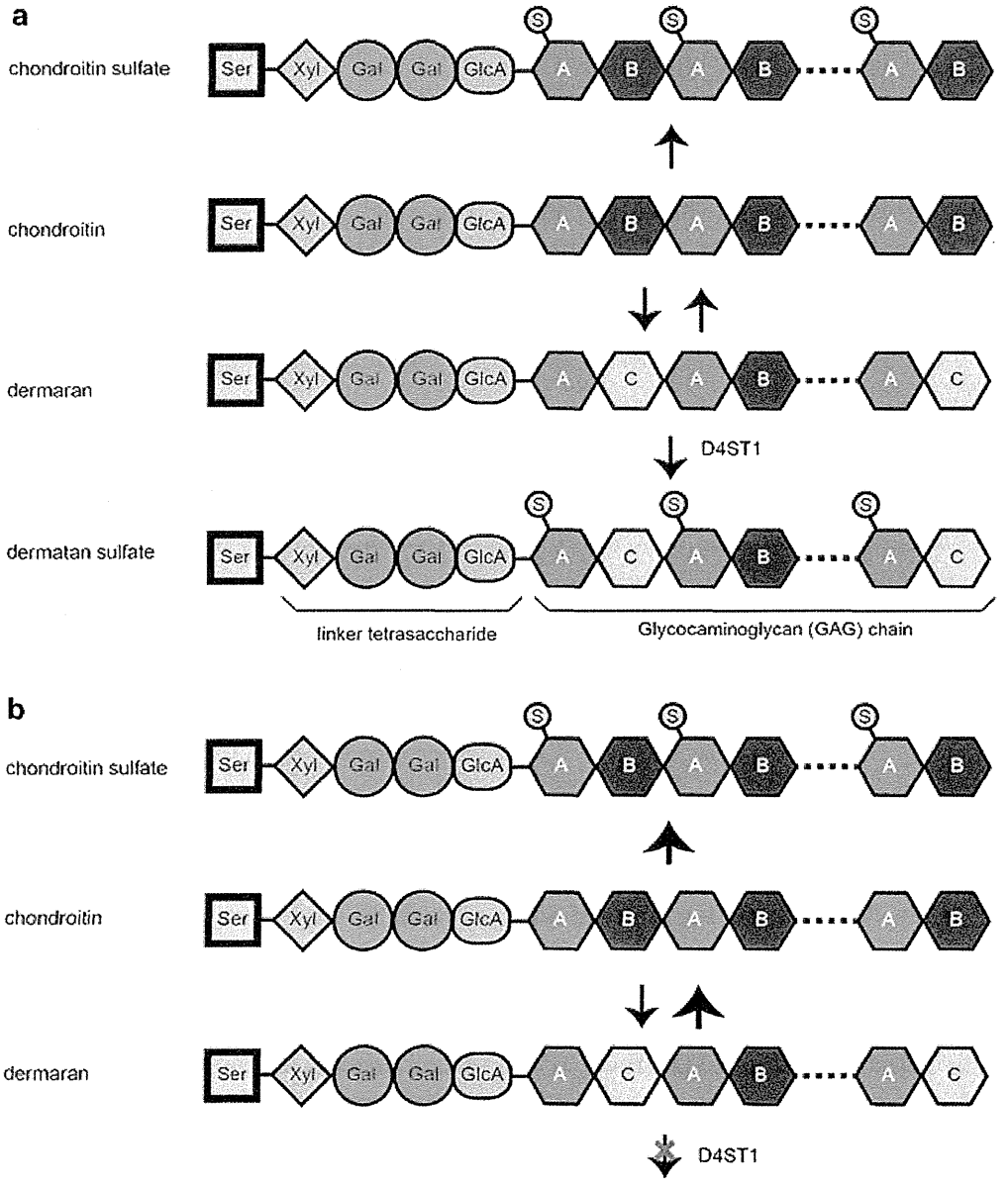

Fig. 10.3 Effects of D4ST1 defects on the biosynthesis of CS and DS. (**a**) The starting structure is chondroitin with a repeating disaccharide consisting of GalNAc [position A] and GlcA [position B]. Sulfation by 6-*O*-GalNAc sulfotransferase and 4-*O*-GalNAc sulfotransferase creates CS from chondroitin. To produce DS, first, C5-carboxy epimerase replaces GlcA with IdoA [position C]. This process is bidirectional as indicated by the bi-directional arrows. Then, D4ST1 adds sulfates to dermatan creating DS and prevents back epimerization. DS is often detected as a CS/DS hybrid. (**b**) In D4ST1-deficient EDS, back epimerization from IdoA to GlcA occurs. Consequently, neither DS nor dermatan are detected in fibroblasts derived from patients. *Gal galactose*, *GlcA* glucuronic acid, *S* active sulfate, *Ser* serine, *Xyl* xylose

short stature, osteopenia of all bones, dysplasia of some bones, and hypotonia. In 2004, Faiyaz-Ul-Haque et al. reported two patients from a large consanguineous Qatari family. The clinical features of both Qatari patients and the Danish patient seemed to be different from those of the original five patients [14].

10.3.2 Genetic Information

10.3.2.1 B4GALT7

In 1999, two different research groups [1, 33] identified compound heterozygous mutations of gene for xylosylprotein beta 1,4-galactosyltransferase, polypeptide 7 (*B4GALT7*, NM_007255.2),

c.557C>A (p.Ala186Asp) and c.617T>C (p.Leu206Pro) in the Danish patient reported by Kresse in 1987 [26]. The two Qatari patients from a large consanguineous family were analyzed in 2004 [14]. Based on the hypothesis of autosomal recessive inheritance, haplotype analysis using microsatellite markers for the limited candidate loci delineated a homozygous region from *D5S469* and *D5S2111*, which harbors *B4GALT7* [14]. A homozygous missense mutation (c.808C>T, p.Arg270Cys) in *B4GALT7* was identified. Interestingly, the clinical phenotype of the Qatari patients was milder than that of the Danish one.

B4GALT7 was cloned by Okajima et al. [34]. The gene consists of six coding exons with a 948-bp open reading frame. This gene encodes xylosylprotein β-1,4-galactosyltransferase, polypeptide 7 (B4GALT7; aliases: galactosyltransferase I, XGPT1, and XGALT1), which is 327 amino acids long and its molecular weight is 37.4 kDa. B4GALT7 is a type II transmembrane protein localized in the Golgi apparatus, and is a key initiator of GAG synthesis as it attaches the first galactose of the linker tetrasaccharide of PGs (Fig. 10.1a, b).

10.3.2.2 B3GALT6

In 2013, Nakajima et al. have identified compound heterozygous mutations of *B3GALT6* (NM_080605.3) in three patients with progeroid form of EDS [32]. This intronless gene has a 990-bp open reading frame and encodes UDP-Gal:βGal β 1,3-galactosyltransferase polypeptide 6 (alternatively galactosyltransferase -II: GalT-II), which is 329 amino acids long and its molecular weight is 37.1kDa. It is also the type II transmembrane protein localized in the Golgi apparatus, and it attaches the second galactose of the tetrasaccharide linker of PGs (Fig. 10.1a, c). So far, two missense (c.16C>T, p.Arg6Trp and c.925T>A, p.Ser309Thr), two frameshift deletions (c.353delA, p.Asp118Alafs*160 and c.588delG, p.Arg197Alafs*81) and one in-frame deletion (c.415_423del, p.Met139Ala141del) were reported in this type of EDS [32].

10.3.3 Biochemical Characteristics

10.3.3.1 B4GALT7

Kresse et al. reported that their patient's fibroblasts produced only PG chain-free core proteins (molecular weight: 46 and 44 kDa) whereas control fibroblasts produced normal PG chains [26]. Additionally, the GAG-free core protein in that patient contained unsubstituted xylose residues (Fig. 10.1b).

Okajima et al. measured the enzyme activity of exogenously expressed proteins (wild type, p.Ala186Asp, p.Leu206Pro) in XGalT-1/B4GALT7-deficient CHO cells [33]. In total cell lysates, the enzyme activity of the p.Ala186Asp mutant was approximately 50 % lower than that of the wild-type protein, whereas the activity of the p.Leu206Pro mutant was almost undetectable. Interestingly, the wild-type and p.Ala186Asp proteins were localized in the Golgi apparatus whereas the p.Leu206Pro mutant existed in the cytoplasm. The α-helix disrupted by p.Leu206Pro may alter the protein's conformation, thus impairing intracellular trafficking and enzyme activity [33].

B4GALT7 activity in fibroblasts from another patient with a homozygous mutation, c.808C>T (p.Arg270Cys), was also lower than that of controls [40]. The extracellular matrix around the B4GALT7^{Arg270Cys} mutant fibroblasts was disorganized without banded fibrils. Furthermore, the proliferation of B4GALT7^{Arg270Cys} fibroblasts was significantly reduced to 45 % of the level of control fibroblasts [40].

Bui et al. measured galactosyltransferase activity of B4GALT7 mutants expressed in CHO pgsB-618 cells using 4-methylumbelliferyl-β-D-xylopyranoside as acceptor substrate. The enzyme activities of the p.Arg270Cys, p.Ala186Asp, and p.Leu206Pro mutants were decreased to 60, 11, and 0 % (undetectable) of that of the wild-type enzyme [4]. It has been reported that the clinical features of patients with the homozygous p.Arg270Cys mutation appear to be milder than those of patients with compound heterozygous mutations, including p.Ala186Asp or p.Leu206Pro, supporting the different effects of these mutations.

10.3.3.2 B3GALT6

Nakajima et al. measured the galactosyltransferase activity of *B3GALT6* in vitro using soluble-FLAG-tagged proteins for wild-type and mutant (p.Ser309Thr) which was observed common in two families and revealed the enzyme activity of the mutant protein was significantly decreased compared to the wild-type [32].

10.4 D4ST1-Deficient EDS (MIM#601776)

Alternative Names
Ehlers–Danlos syndrome, type VIB, formerly
Ehlers–Danlos syndrome, Kosho type
Ehlers–Danlos syndrome, musculocontractural type
Adducted thumbs, clubfoot, and progressive joints and skin laxity syndrome
Adducted thumb-clubfoot syndrome (ATCS)
Dündar syndrome
Arthrogryposis, distal, with peculiar faces and hydronephrosis

10.4.1 Clinical Manifestations

The kyphoscoliosis type of EDS (formerly known as, EDS type VI) is characterized by generalized joint laxity, severe muscular hypotonia and scoliosis at birth, scleral fragility, and rupture of the ocular globe [2]. This disorder is essentially caused by lysyl hydroxylase deficiency (EDS type VIA); other patients with similar clinical manifestations but without lysyl hydroxylase deficiency were classified as EDS type VIB.

In 2005, Kosho et al. reported two unrelated patients with fragile and hyperextensible skin, a high propensity for bruising, generalized joint laxity, kyphoscoliosis, and the major features of EDS VI, as well as a characteristic craniofacial appearance, and multiple congenital contractures [25]. Lysyl hydroxylase deficiency was excluded in these patients by analysis of the urinary deoxypyridinoline:pyridinoline ratio, and the patients were tentatively classified as EDS VIB. Kosho et al. subsequently reported on four additional unrelated patients and concluded that the patients represented a new type of EDS [23]. Notably, all six patients had homozygous or compound heterozygous mutations in *CHST14* [31]. Loss-of-function mutations in *CHST14* were independently found in 11 patients from four families with a rare arthrogryposis syndrome known as "adducted thumb-clubfoot syndrome (ATCS)" [9–11, 21, 43] and in three patients from two families who were originally classified as suffering from EDS VIB [27]. Malfait et al. suggested that these patients had the same disorder, which they termed "musculocontractural EDS" [27]. Shimizu et al. described the clinical characteristics of two additional patients together with a review of all of the patients reported at that time; their findings support the notion that the three independently identified conditions represent a single type of EDS [41]. Conversely, Janecke et al. claimed that the disorder should not be categorized as a type of EDS because of the presence of atypical clinical features, including facial dysmorphism, multiple congenital contractures, visceral anomalies, and impaired biosynthesis of DS as a cause of the disorder, and proposed the term DS-deficient adducted thumb-clubfoot syndrome [20]. In their response, Kosho et al. provided clinical and etiological evidence from which the disorder could be categorized as a type of EDS, because of the presence of all major features of EDS, including connective tissue fragility which required special and appropriate management of these patients. Decorin-mediated impaired assembly of collagen fibrils was the primary cause of progressive connective tissue fragility in this type [24]. Therefore, Kosho et al. proposed that the term D4ST1-deficient EDS (adducted thumb-clubfoot syndrome) was appropriate for this syndrome [24]. The current OMIM (http://www.ncbi.nlm.nih.gov/omim) registration of this disorder is EDS, musculocontractural type.

To date, descriptions of 26 patients (12 males, 14 females) from 17 families have been published [9–11, 21, 23, 25, 27, 30, 31, 41, 43, 46,

Table 10.1 Classification of Ehlers-Danlos syndrome

	Prevalence/patient number	Inheritance	Causative gene
Major types			
Classical type	1/20,000	AD	*COL5A1, COL5A2*
Hypermobility type	1/5,000–20,000	AD	Unknown[a]
Vascular type	1/50,000–250,000	AD	*COL3A1*
Kyphoscoliosis type	1/100,000	AR	*PLOD1*
Arthrochalasia type	30	AD	*COL1A1, COL1A2*
Dermatosparaxis type	8	AR	*ADAMTS2*
Other types			
Brittle cornea syndrome	11	AR	*ZNF469*
EDS-like syndrome due to tenascin-XB deficiency	10	AR	*TNXB*
Progeroid form	7	AR	*B4GALT7, B3GALT6*
Cardiac valvular form	4	AR	*COL1A2*
EDS-like spondylocheirodysplasia	8	AR	*SLC39A13*
D4ST1-deficient EDS (DD-EDS)	22	AR	*CHST14*

AD, autosomal dominant; *AR*, autosomal recessive; *COL5A1*, collagen, type V, alpha 1; *COL5A2*, collagen, type V, alpha 2; *COL3A1*, collagen, type III, alpha 1; *PLOD1*, procollagen-lysine, 2-oxoglutarate 5-dioxygenase 1; *COL1A1*, collagen, type I, alpha 1; *COL1A2*, collagen, type I, alpha 2; *ADAMTS2*, ADAM metallopeptidase with thrombospondin type 1 motif, 2; *ZNF469*, zinc finger protein 469; *TNXB*, tenascin XB; *B4GALT7*, xylosylprotein beta 1,4-galactosyltransferase, polypeptide 7; *B3GALT6*, UDP-Gal:βGal β 1,3-galactosyltransferase polypeptide 6; *COL1A2*, collagen, type I, alpha 2; *SLC39A13*, solute carrier family 39 (zinc transporter), member 13; *CHST14*, carbohydrate (*N*-acetylgalactosamine 4-*0*) sulfotransferase 14

[a] *TNXB* mutations in a small subset of patients

48, 49]. This syndrome is characterized by a unique set of clinical features consisting of progressive systemic manifestations, including tissue fragility (e.g., skin hyperextensibility and fragility, progressive spinal and foot deformities, and large subcutaneous hematomas) and various malformations (e.g., facial features, congenital eye/heart/gastrointestinal defects, congenital multiple contractures). We have summarized the main clinical features of this syndrome in each organ in Table 10.1

10.4.1.1 Craniofacial Features

The characteristic craniofacial features apparent at birth or during early infancy include a large fontanelle, hypertelorism, short and down slanting palpebral fissures, blue sclerae, a short nose with hypoplastic columella, low-set and rotated ears, a high or cleft palate, a long philtrum, a thin upper-lip vermilion, a small mouth, and micro-retrognathia (Fig. 10.4a, b). Slender and asymmetrical facial shapes with a protruding jaw are generally observed from school age onwards (Fig. 10.4c, d).

10.4.1.2 Skeletal Features

Congenital multiple contractures, particularly adduction-flexion contractures of the thumbs and talipes equinovarus, are the main skeletal features (Fig. 10.4e, g, h). Fingers with a "tapering", "slender", and "cylindrical" shape are also common (Fig. 10.4f). Aberrant finger movement was described in three patients. Four patients had tendon abnormalities, including anomalous insertion of the flexor muscles, which probably caused the congenital contractures. Spinal deformities (e.g., scoliosis and kyphoscoliosis) and talipes deformities (e.g., planus and valgus) (Fig. 10.4i) occurred and progressed during childhood. Marfanoid habitus, recurrent joint dislocations, and pectus deformities (e.g., flat and thin, excavatum, and carinatum) were also evident. Bone mineral density was decreased in five patients and normal in two. Urine concentrations of the N-telopeptide of collagen type I, an osteoclast marker, were increased in three patients, whereas serum bone-specific alkaline phosphatase concentrations, an osteoblast marker, were normal in three, suggesting that

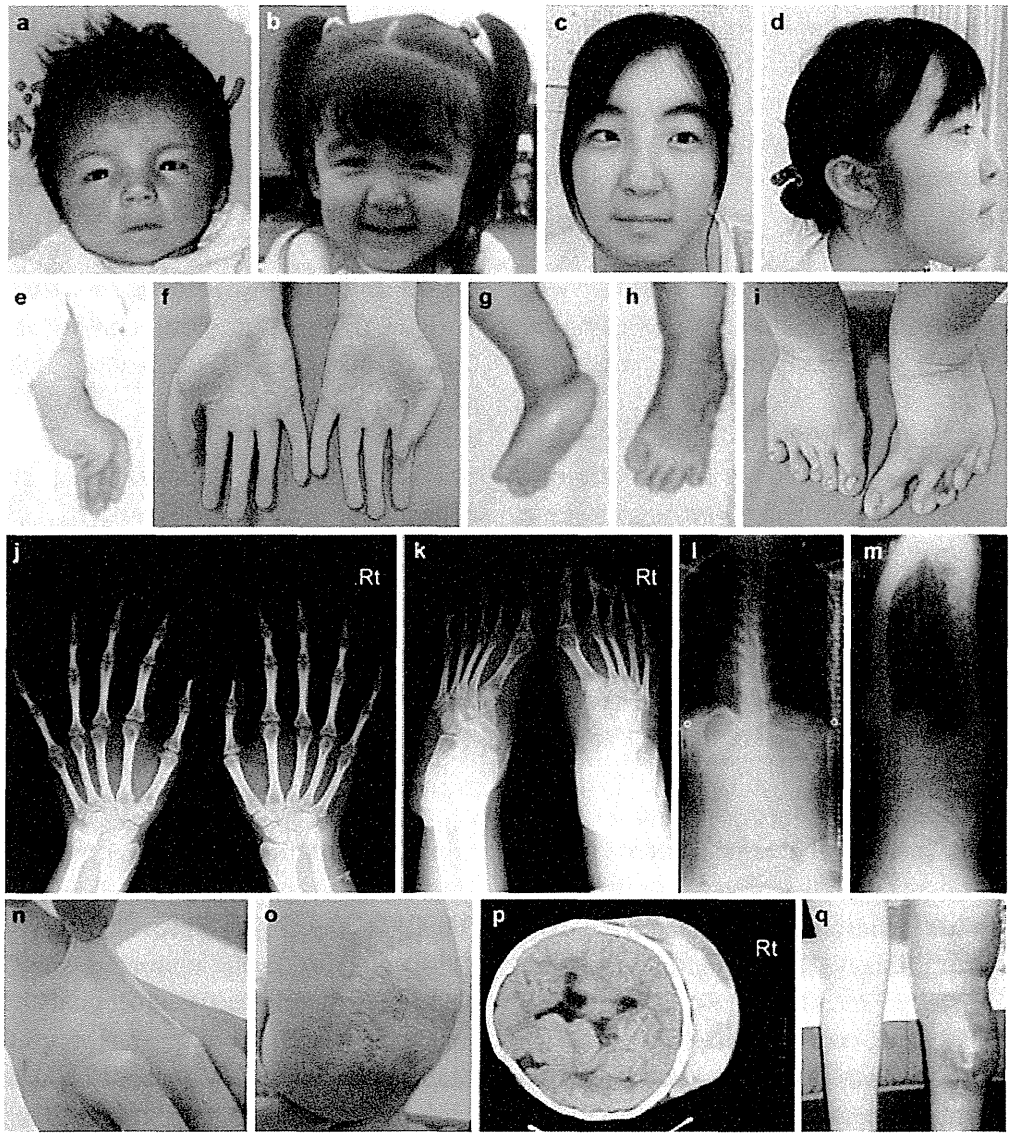

Fig. 10.4 Clinical photographs of patients with D4ST1-deficient EDS. (**a–d**) Facial features of a patient at 23 days (**a**), 3 years (**b**), and 16 years (**c**, **d**) of age. (**e**, **f**) Images of the hand in a patient with an adducted thumb at 1 month of age (**e**) and cylindrical fingers at 19 years of age (**f**). (**g–i**) Images of the foot in a patient with bilateral clubfeet at 1 month of age (**g**, **h**) and progressive talipes deformities (planus and valgus) at 19 years of age (**i**). (**j–m**) Radiographs of a 16-year-old patient show diaphyseal narrowing of the phalanges and metacarpals (**j**, **k**) and kyphoscoliosis with tall vertebral bodies (**l**, **m**). (**n**, **o**) Cutaneous features of a 19-year-old patient with hyperextensibility (**n**), atrophic scars, and fistula formation (**o**). (**p**) A massive cranial subcutaneous hematoma in the head of a 6-year-old patient after falling onto the floor. (**q**) A subcutaneous hematoma in the leg of a 16-year-old patient (All figures were originally published in Kosho et al. [23] except Fig. 10.4p, which was published in Kosho et al. [25])

increased osteoclast activity but normal osteoblast activity could cause osteopenia or osteoporosis. Radiologically, diaphyseal narrowing of the phalanges and metacarpals was noted in six patients (Fig. 10.4j, k). Talipes valgus and planus or cavum, with diaphyseal narrowing of the phalanges and metatarsals, were noted in six patients. Tall vertebral bodies were noted in five patients (Fig. 10.4l, m).

10.4.1.3 Cutaneous Features

Cutaneous features were apparent in most patients, including hyperextensibility to redundancy (Fig. 10.4n), a high propensity for bruising,

fragility leading to atrophic scars (Fig. 10.4o), acrogeria-like fine palmar creases or wrinkles, hyperalgesia to pressure, and recurrent subcutaneous infections with fistula formation. The palmar creases increased and became deeper with age.

10.4.1.4 Cardiovascular Features

Large subcutaneous hematomas were common, and frequently required intensive treatment, including hospital admission, blood transfusion, and surgical drainage (Fig. 10.4p, q). The lesions were thought to be caused by the rupture of a subcutaneous artery or vein. Bleeding time was prolonged in two patients (9 min and 11 min) and was normal in three. Intranasal administration of 1-desamino-8-D-arginine vasopressin prevented the development of large subcutaneous hematomas after trauma [49]. Four patients had congenital heart defects including an atrial septal defect in three, a patent ductus arteriosus in one, and coarctation of the aorta in one. Five patients had cardiac valve abnormalities including one who underwent surgery for infectious endocarditis, which was probably caused by aortic valve or mitral valve regurgitation.

10.4.1.5 Respiratory Features

Three adult patients developed pneumothorax or hemopneumothorax requiring chest tube drainage.

10.4.1.6 Gastrointestinal Features

Numerous gastrointestinal abnormalities were reported, including diverticular perforation in two adult patients, constipation in seven patients, abdominal pain in two patients, and other disorders in one patient (common mesentery, absence of the gastrocolic omentum with a spontaneous volvulus of small intestine, gastric ulcer, and malrotation with duodenal obstruction).

10.4.1.7 Genitourinary Features

Urological complications included nephrolithiasis or cystolithiasis in five patients, hydronephrosis in three, a dilated or atonic bladder with recurrent urinary tract infection in two, and a horseshoe kidney in one. Cryptorchidism was observed in eight male patients, including one who underwent orchiopexy because of hypogonadism in adulthood. Poor breast development was noted in five adolescent or adult patients. No pregnant females have been reported.

10.4.1.8 Ophthalmologic Features

Various ophthalmological complications have been reported, including strabismus in 12 patients, refractive errors in nine, glaucoma or elevated intraocular pressure in six, microcornea or microphthalmia in three, and retinal detachment in three.

10.4.1.9 Hearing Impairment

Six patients had hearing impairments, including for high-pitched sounds in three.

10.4.1.10 Growth

Patients showed mild prenatal growth retardation as the mean birth length was −0.5 standard deviations (SD), the mean birth weight was −0.6 SD, and the mean birth occipitofrontal circumference (OFC) was −0.2 SD. Postnatal growth was also mildly impaired, as the patients were generally slender with relative macrocephaly. The mean height was −0.9 SD, the mean weight was −1.5 SD, and the mean OFC was −0.2 SD.

10.4.1.11 Development and Neuromuscular Features

Gross motor developmental delay was observed in 14 patients, as the median age of independent walking was 2 years 1 month. Two patients, aged 15 years and 32 years, could not walk unassisted. An underlying myopathic process was observed in two patients. Mild intellectual disability was apparent in four patients. One patient had a global psychomotor delay at 1.5 years of age, but his intellectual quotient was approximately 90 at the age of 7 years 2 months. Brain imaging showed ventricular enlargement and/or asymmetry in seven patients, absence of the left septum pellucidum in one patient, and a short corpus callosum, mildly prominent Sylvian fissures, and periventricular nodular heterotopias. Two patients had spinal cord tethering.

10.4.2 Genetic Information

Autosomal recessive inheritance was considered based on the presence of this syndrome in consanguineous families [11, 27, 31]. Three independent groups have performed homozygosity mapping and/or linkage analysis and each showed that the gene carbohydrate (*N*-acetylgalactosamine 4-*O*) sulfotransferase 14 (*CHST14*, NM_130468.3) was responsible for this syndrome [11, 27, 31].

The *CHST14* gene was first cloned by Evers et al. [13]. It contains one coding exon (1,131-bp open reading frame) and is localized at 15q15.1. This gene encodes D4ST1, a 376 amino acid type II transmembrane protein (molecular weight: 43 kDa), that is localized in the Golgi membrane. It transfers a sulfate group from 3′-phosphoadenosine 5′-phosphosulfate to position 4 of the GalNAc residues in dermatan to generate DS (Figs. 10.1a and 10.3a). Northern blotting revealed that *CHST14* is mainly expressed in heart, placenta, liver, and pancreas, and is weakly expressed in lung, skeletal muscle, and kidney [13].

To date, 11 pathogenic mutations of *CHST14* have been identified: p.Val49*, p.Lys69*, p.Arg135_Leu137delinsGlyThrGln, p.Phe209Ser, p.Arg213Pro, p.Lys226Alafs*16, p.Arg274Pro, p.Pro281Leu, p.Cys289Ser, p.Tyr293Cys, and p.Glu334Glyfs*107 [11, 27, 30, 31, 46, 48]. (p.Val48* was corrected to p.Val49*; Erratum in Am J Med Genet Part A 161A(2):403 (2013)) (p.Arg135Gly and p.Leu137Gln were originally reported by Dündar et al., but lately registered as c.403_410delCGCACCCTinsGGCACCCA, p.Arg135_Leu137delinsGlyThrGln in The Human Gene Mutation Database: https://portal.biobase-international.com/hgmd/pro/genesearch.php). Because these are protein truncation mutations and missense mutations, it seems likely that the mutations cause a loss of function.

10.4.3 Biochemical Information

Dündar et al. reported that DS-derived IdoA-GalNAc(4S) disaccharide was undetectable in fibroblasts derived from a patient with a homozygous p.Arg213Pro mutation. They also reported that GlcA-GalNAc(4S) content was greatly increased in the fibroblast extract and the culture media obtained from cultures of fibroblasts derived from this patient as compared with control fibroblasts [11]. It was also found that the amount of nonsulfated disaccharides (GlcA-GalNAc and IdoA-GalNAc) was increased in the cell extract and its media from the patient's fibroblast as compared with normal control fibroblasts. From these results, Dündar et al. proposed that epimerization of GlcA to IdoA by C5-carboxy epimerase is followed by sulfation of the C4 hydroxyl on the adjacent GalNAc residue by D4ST1. This process generates DS from dermatan and prevents back-epimerization from IdoA to GlcA [11, 28].

Miyake et al. measured the sulfotransferase activity of COS7 cells transfected with wild-type and mutant D4ST1 harboring the p.Lys69*, p.Pro281Leu, p.Cys289Ser, or p.Tyr293Cys mutations. The enzyme activity of the mutants was as low as that in mock transfected cells, suggesting that these missense mutations result in the loss of function [31]. The disaccharide composition of the decorin GAG chain isolated from the patient's fibroblasts consisted only of CS, without DS, while the chains isolated from normal fibroblasts consisted of CS/DS hybrid chains [31]. Furthermore, the level of nonsulfated dermatan was negligible in the patient's fibroblasts [31]. Thus, in this syndrome, the CS/DS chain is replaced with the CS chain, even though the core proteins are normal.

10.4.4 Pathology and Pathophysiology

Of the major DS proteoglycans in skin, decorin was a focus of research because it binds to collagen fibrils via its core protein and its GAG chains act as interfibrillar bridges [38, 39]. Three α collagen chains are self-assembled to generate tropocollagen, in the form of a triple helix. Tropocollagen then self-assembles to form collagen fibrils via decorin (Fig. 10.5a). Collagen fibrils are assembled into a collagen fiber, known as the collagen bundle, via the antiparallel com-

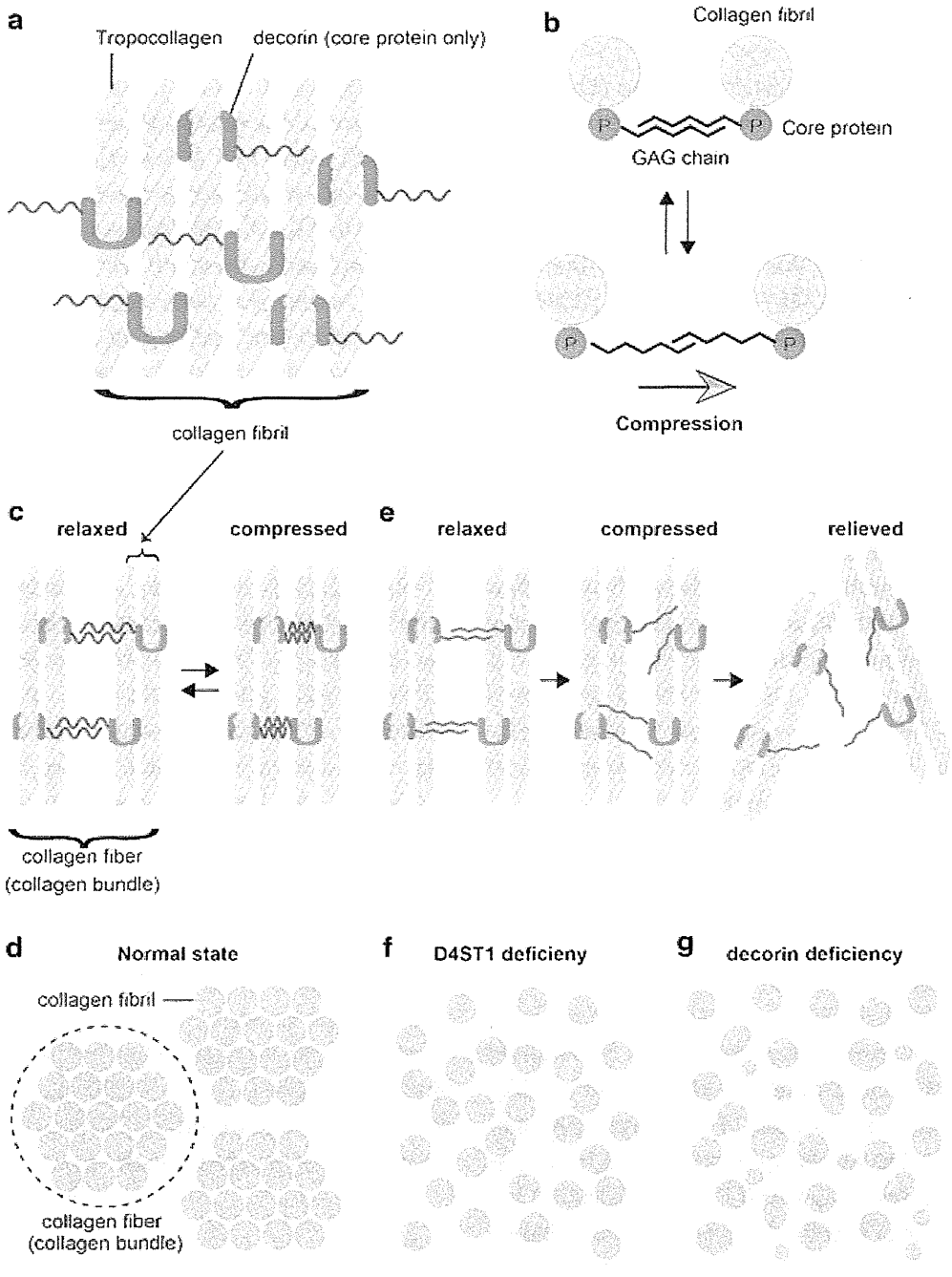

Fig. 10.5 Putative model of abnormal collagen bundle assembly in D4ST1-deficient EDS. (**a**) Tropocollagen directly binds to decorin and forms a collagen fibril. The *blue lines* represent the CS/DS hybrid chain. (**b**) Illustration of the sliding filament model showing reversible longitudinal slippage between the antiparallel GAG chains. The *black lines* represent unspecified GAGs. (**c, d**) In the normal state, the CS/DS chains can bend against the direction of mechanical compression and rebound to the original structure (**c**). Thus, the collagen bundles are refractory to compression stress (**d**). (**e, f**) In D4ST1-deficient EDS, the CS/DS chains are replaced with CS chains (*red lines*). These chains cannot resist mechanical compression, resulting in irreversible scattering of the collagen fibrils. (**g**) The size and shape of the collagen fibrils are highly variable in decorin-deficient mice

plex of the CS/DS hybrid GAG chains of decorin, which acts like a bridge to provide a space between individual fibrils and tighten the collagen fiber (Fig. 10.5c, d).

The GAGs span collagen fibrils in the extracellular matrix of skin and tendons, and the length of the GAG chain determines the width of the interfibrillar gap [35, 36]. Elasticity of the

extracellular matrix is explained by the sliding filament model, which allows reversible longitudinal slippage between the antiparallel GAG chains (Fig. 10.5b) [39]. Because tissue stability and elasticity depend on the structure of the GAG bridges, irreversible damage can occur if the bridges are inelastic [39].

Decorin is composed of a horseshoe-shaped core protein (molecular weight: ~45 kDa) and a single CS/DS hybrid chain on the N-terminal side (Fig. 10.5a) [22, 47]. Weber et al. reported that the model structure of decorin consists of an arch in which the inner concave surface is formed from a curved β-sheet and the outer convex surface is formed from α-helices. They also proposed that one tropocollagen fiber lies within the decorin convex and another interacts with one arm of the arch [47]. The IdoA:GlcA ratio in DS ranges from ~10 to >90 % depending on the tissue type [39]. Importantly, L-IdoA residues in DS can easily undergo conformational changes, unlike GlcA in CS [6, 7]. Thus, the IdoA:GlcA ratio should be higher in more flexible tissues [39].

Light microscopic investigation of skin specimens from two patients showed that fine collagen fibers were predominant in the reticular to papillary dermis and the number of thick collagen bundles was markedly reduced [31]. Electron microscopic examination of the specimens showed that collagen fibrils were dispersed throughout the reticular dermis, whereas they were regularly and tightly assembled in control tissue. Surprisingly, each collagen fibril was smooth and round, with little variation in size or shape, similar to the fibril in the control tissue (Fig. 10.5d, f) [31]. The disaccharide composition of the decorin GAG chain from a patient's fibroblasts only consisted of CS, without DS disaccharide, whereas control fibroblasts consisted of a CS/DS hybrid [31]. The transition of decorin from the CS/DS hybrid chain to a CS chain probably decreases the flexibility of the GAG chain. The sliding filament model proposes that mechanical compression might also work in the CS chain of D4ST1-deficient patients, but the inflexibility of the CS chain is unable to tolerate higher mechanical pressures or is too inelastic to maintain normal skin properties (Fig. 10.5e, f). This irreversible event could explain the progressive clinical course of this disease.

Interestingly, there were marked variations in the size and shape of dermal collagen fibrils in decorin-null mice (Fig. 10.5g) [8]. These findings suggest that the decorin core protein is important for collagen fibril formation, and that the CS/DS hybrid chain of decorin PG regulates the space between the collagen fibrils and form collagen bundles, as previously reported [37]. These findings suggest that the main pathological basis of this disorder could be insufficient assembly of collagen fibrils.

However, Dündar et al. reported that the light microscopic and electron microscopic findings of a patient's skin were unchanged compared to the normal control [11]. Malfait et al. reported that, in their patient, most collagen bundles were small diameter in size, and some were composed of collagen fibrils of varying diameter that were separated by irregular interfibrillar spaces [27]. In addition, the fibroblasts exhibited an elongated and/or dilated endoplasmic reticulum. So far, definitive histopathologic characteristics have not been established, so further studies are strongly encouraged to determine the major histological characteristics and underlying pathophysiology of this disorder.

References

1. Almeida R, Levery SB, Mandel U, Kresse H, Schwientek T, Bennett EP, Clausen H (1999) Cloning and expression of a proteoglycan UDP-galactose:beta-xylose beta1,4-galactosyltransferase I. A seventh member of the human beta4-galactosyltransferase gene family. J Biol Chem 274:26165–26171
2. Beighton P, De Paepe A, Steinmann B, Tsipouras P, Wenstrup RJ (1998) Ehlers-Danlos syndromes: revised nosology, Villefranche, 1997. Ehlers-Danlos National Foundation (USA) and Ehlers-Danlos Support Group (UK). Am J Med Genet 77:31–37
3. Bishop JR, Schuksz M, Esko JD (2007) Heparan sulphate proteoglycans fine-tune mammalian physiology. Nature 446:1030–1037
4. Bui C, Talhaoui I, Chabel M, Mulliert G, Coughtrie MW, Ouzzine M, Fournel-Gigleux S (2010) Molecular characterization of beta1,4-galactosyltransferase 7 genetic mutations linked to the progeroid form of Ehlers-Danlos syndrome (EDS). FEBS Lett 584:3962–3968
5. Bulow HE, Hobert O (2006) The molecular diversity of glycosaminoglycans shapes animal development. Ann Rev Cell Dev Biol 22:375–407
6. Casu B, Petitou M, Provasoli M, Sinay P (1988) Conformational flexibility: a new concept for explaining binding and biological properties of iduronic acid-

containing glycosaminoglycans. Trends Biochem Sci 13:221–225
7. Catlow KR, Deakin JA, Wei Z, Delehedde M, Fernig DG, Gherardi E, Gallagher JT, Pavao MS, Lyon M (2008) Interactions of hepatocyte growth factor/scatter factor with various glycosaminoglycans reveal an important interplay between the presence of iduronate and sulfate density. J Biol Chem 283:5235–5248
8. Danielson KG, Baribault H, Holmes DF, Graham H, Kadler KE, Iozzo RV (1997) Targeted disruption of decorin leads to abnormal collagen fibril morphology and skin fragility. J Cell Biol 136:729–743
9. Dündar M, Demiryilmaz F, Demiryilmaz I, Kumandas S, Erkilic K, Kendirci M, Tuncel M, Ozyazgan I, Tolmie JL (1997) An autosomal recessive adducted thumb-club foot syndrome observed in Turkish cousins. Clin Genet 51:61–64
10. Dündar M, Kurtoglu S, Elmas B, Demiryilmaz F, Candemir Z, Ozkul Y, Durak AC (2001) A case with adducted thumb and club foot syndrome. Clin Dysmorphol 10:291–293
11. Dündar M, Müller T, Zhang Q, Pan J, Steinmann B, Vodopiutz J, Gruber R, Sonoda T, Krabichler B, Utermann G, others (2009) Loss of dermatan-4-sulfotransferase 1 function results in adducted thumb-clubfoot syndrome. Am J Hum Genet 85:873–882
12. Esko JD, Kimata K, Lindahl U (2009) Proteoglycans and sulfated glycosaminoglycans. In: Varki A, Cummings RD, Esko JD, Freeze HH, Stanley P, Bertozzi CR, Hart GW, Etzler ME (eds) Essentials of glycobiology. Cold Spring Harbor, New York
13. Evers MR, Xia G, Kang HG, Schachner M, Baenziger JU (2001) Molecular cloning and characterization of a dermatan-specific N-acetylgalactosamine 4-O-sulfotransferase. J Biol Chem 276:36344–36353
14. Faiyaz-Ul-Haque M, Zaidi SH, Al-Ali M, Al-Mureikhi MS, Kennedy S, Al-Thani G, Tsui LC, Teebi AS (2004) A novel missense mutation in the galactosyltransferase-I (B4GALT7) gene in a family exhibiting facioskeletal anomalies and Ehlers-Danlos syndrome resembling the progeroid type. Am J Med Genet Part A 128A:39–45
15. Freeze HH (2006) Genetic defects in the human glycome. Nat Rev Genet 7:537–551
16. Hernandez A, Aguirre-Negrete MG, Gonzalez-Flores S, Reynoso-Luna MC, Fragoso R, Nazara Z, Tapia-Arizmendi G, Cantu JM (1986) Ehlers-Danlos features with progeroid facies and mild mental retardation. Further delineation of the syndrome. Clin Genet 30:456–461
17. Hernandez A, Aguirre-Negrete MG, Liparoli JC, Cantu JM (1981) Third case of a distinct variant of the Ehlers-Danlos Syndrome (EDS). Clin Genet 20:222–224
18. Hernandez A, Aguirre-Negrete MG, Ramirez-Soltero S, Gonzalez-Mendoza A, Martinez y Martinez R, Velazquez-Cabrera A, Cantu JM (1979) A distinct variant of the Ehlers-Danlos syndrome. Clin Genet 16:335–339
19. Jaeken J, Hennet T, Freeze HH, Matthijs G (2008) On the nomenclature of congenital disorders of glycosylation (CDG). J Inherit Metab Dis 31:669–672
20. Janecke AR, Baenziger JU, Müller T, Dündar M (2011) Loss of dermatan-4-sulfotransferase 1 (D4ST1/CHST14) function represents the first dermatan sulfate biosynthesis defect, "dermatan sulfate-deficient adducted thumb-club-foot syndrome". Hum Mutat 32:484–485
21. Janecke AR, Unsinn K, Kreczy A, Baldissera I, Gassner I, Neu N, Utermann G, Müller T (2001) Adducted thumb-club foot syndrome in sibs of a consanguineous Austrian family. J Med Genet 38:265–269
22. Kobe B, Deisenhofer J (1993) Crystal structure of porcine ribonuclease inhibitor, a protein with leucine-rich repeats. Nature 366:751–756
23. Kosho T, Miyake N, Hatamochi A, Takahashi J, Kato H, Miyahara T, Igawa Y, Yasui H, Ishida T, Ono K, others (2010) A new Ehlers-Danlos syndrome with craniofacial characteristics, multiple congenital contractures, progressive joint and skin laxity, and multisystem fragility-related manifestations. Am J Med Genet Part A 152A:1333–1346
24. Kosho T, Miyake N, Mizumoto S, Hatamochi A, Fukushima Y, Yamada S, Sugahara K, Matsumoto N (2011) A response to: loss of dermatan-4-sulfotransferase 1 (D4ST1/CHST14) function represents the first dermatan sulfate biosynthesis defect, "dermatan sulfate-deficient Adducted Thumb-Clubfoot Syndrome". Which name is appropriate, "Adducted Thumb-Clubfoot Syndrome" or "Ehlers-Danlos syndrome"? Hum Mutat 32:1507–1509
25. Kosho T, Takahashi J, Ohashi H, Nishimura G, Kato H, Fukushima Y (2005) Ehlers-Danlos syndrome type VIB with characteristic facies, decreased curvatures of the spinal column, and joint contractures in two unrelated girls. Am J Med Genet Part A 138A:282–287
26. Kresse H, Rosthoj S, Quentin E, Hollmann J, Glossl J, Okada S, Tonnesen T (1987) Glycosaminoglycan-free small proteoglycan core protein is secreted by fibroblasts from a patient with a syndrome resembling progeroid. Am J Hum Genet 41:436–453
27. Malfait F, Syx D, Vlummens P, Symoens S, Nampoothiri S, Hermanns-Le T, Van Laer L, De Paepe A (2010) Musculocontractural Ehlers-Danlos Syndrome (former EDS type VIB) and adducted thumb clubfoot syndrome (ATCS) represent a single clinical entity caused by mutations in the dermatan-4-sulfotransferase 1 encoding CHST14 gene. Hum Mutat 31:1233–1239
28. Malmström A (1984) Biosynthesis of dermatan sulfate. II. Substrate specificity of the C-5 uronosyl epimerase. J Biol Chem 259:161–165
29. Mao JR, Bristow J (2001) The Ehlers-Danlos syndrome: on beyond collagens. J Clin Invest 107:1063–1069
30. Mendoza-Londono R, Chitayat D, Kahr WH, Hinek A, Blaser S, Dupuis L, Goh E, Badilla-Porras R, Howard A, Mittaz L, others (2012) Extracellular matrix and platelet function in patients with musculo-

contractural Ehlers-Danlos syndrome caused by mutations in the CHST14 gene. Am J Med Genet Part A 158A:1344–1354
31. Miyake N, Kosho T, Mizumoto S, Furuichi T, Hatamochi A, Nagashima Y, Arai E, Takahashi K, Kawamura R, Wakui K, others (2010) Loss-of-function mutations of CHST14 in a new type of Ehlers-Danlos syndrome. Hum Mutat 31:966–974
32. Nakajima M, Mizumoto S, Miyake N, Kogawa R, Iida A, Ito H, Kitoh H, Hirayama A, Mitsubuchi H, Miyazaki O, others (2013) Mutations in B3GALT6, which encodes a glycosaminoglycan linker region enzyme, cause a spectrum of skeletal and connective tissue disorders. Am J Hum Genet 92:927–934
33. Okajima T, Fukumoto S, Furukawa K, Urano T (1999) Molecular basis for the progeroid variant of Ehlers-Danlos syndrome. Identification and characterization of two mutations in galactosyltransferase I gene. J Biol Chem 274:28841–28844
34. Okajima T, Yoshida K, Kondo T, Furukawa K (1999) Human homolog of Caenorhabditis elegans sqv-3 gene is galactosyltransferase I involved in the biosynthesis of the glycosaminoglycan-protein linkage region of proteoglycans. J Biol Chem 274:22915–22918
35. Scott JE (1988) Proteoglycan-fibrillar collagen interactions. Biochem J 252:313–323
36. Scott JE (1992) Morphometry of cupromeronic blue-stained proteoglycan molecules in animal corneas, versus that of purified proteoglycans stained in vitro, implies that tertiary structures contribute to corneal ultrastructure. J Anat 180(Pt 1):155–164
37. Scott JE (1995) Extracellular matrix, supramolecular organisation and shape. J Anat 187(Pt 2):259–269
38. Scott JE (1996) Proteodermatan and proteokeratan sulfate (decorin, lumican/fibromodulin) proteins are horseshoe shaped. Implications for their interactions with collagen. Biochemistry 35:8795–8799
39. Scott JE (2003) Elasticity in extracellular matrix 'shape modules' of tendon, cartilage, etc. A sliding proteoglycan-filament model. J Physiol 553:335–343
40. Seidler DG, Faiyaz-Ul-Haque M, Hansen U, Yip GW, Zaidi SH, Teebi AS, Kiesel L, Gotte M (2006) Defective glycosylation of decorin and biglycan, altered collagen structure, and abnormal phenotype of the skin fibroblasts of an Ehlers-Danlos syndrome patient carrying the novel Arg270Cys substitution in galactosyltransferase I (beta4GalT-7). J Mol Med (Berl) 84:583–594
41. Shimizu K, Okamoto N, Miyake N, Taira K, Sato Y, Matsuda K, Akimaru N, Ohashi H, Wakui K, Fukushima Y, others (2011) Delineation of dermatan 4-O-sulfotransferase 1 deficient Ehlers-Danlos syndrome: observation of two additional patients and comprehensive review of 20 reported patients. Am J Med Genet Part A 155A:1949–1958
42. Sisu E, Flangea C, Serb A, Zamfir AD (2011) Modern developments in mass spectrometry of chondroitin and dermatan sulfate glycosaminoglycans. Amino Acids 41:235–256
43. Sonoda T, Kouno K (2000) Two brothers with distal arthrogryposis, peculiar facial appearance, cleft palate, short stature, hydronephrosis, retentio testis, and normal intelligence: a new type of distal arthrogryposis? Am J Med Genet 91:280–285
44. Steinmann B, Royce PM, Superti-Furga A (2002) The Ehlers -Danlos syndrome. In: Royce PM and Steinmann B (eds) Connective tissue and its heritable disorders. (2nd edition) Wiley-Liss, Inc., New York
45. Sugahara K, Mikami T, Uyama T, Mizuguchi S, Nomura K, Kitagawa H (2003) Recent advances in the structural biology of chondroitin sulfate and dermatan sulfate. Curr Opin Struct Biol 13:612–620
46. Voermans NC, Kempers M, Lammens M, van Alfen N, Janssen MC, Bonnemann C, van Engelen BG, Hamel BC (2012) Myopathy in a 20-year-old female patient with D4ST-1 deficient Ehlers-Danlos syndrome due to a homozygous CHST14 mutation. Am J Med Genet Part A 158A:850–855
47. Weber IT, Harrison RW, Iozzo RV (1996) Model structure of decorin and implications for collagen fibrillogenesis. J Biol Chem 271:31767–31770
48. Winters KA, Jiang Z, Xu W, Li S, Ammous Z, Jayakar P, Wierenga KJ (2012) Re-assigned diagnosis of D4ST1-deficient Ehlers-Danlos syndrome (adducted thumb-clubfoot syndrome) after initial diagnosis of Marden-Walker syndrome. Am J Med Genet A 158A:2935–2940
49. Yasui H, Adachi Y, Minami T, Ishida T, Kato Y, Imai K (2003) Combination therapy of DDAVP and conjugated estrogens for a recurrent large subcutaneous hematoma in Ehlers-Danlos syndrome. Am J Hematol 72:71–72

CLINICAL REPORT

AMERICAN JOURNAL OF medical genetics PART A

A Novel *WTX* Mutation in a Female Patient With Osteopathia Striata With Cranial Sclerosis and Hepatoblastoma

Atsushi Fujita,[1] Nobuhiko Ochi,[2] Hidehiko Fujimaki,[3] Hideki Muramatsu,[4] Yoshiyuki Takahashi,[4] Jun Natsume,[4] Seiji Kojima,[4] Mitsuko Nakashima,[1] Yoshinori Tsurusaki,[1] Hirotomo Saitsu,[1] Naomichi Matsumoto,[1]* and Noriko Miyake[1]*

[1]Department of Human Genetics, Yokohama City University Graduate School of Medicine, Yokohama, Japan

[2]Department of Pediatrics, Aichi Prefectural Rehabilitation Center for Children with Disabilities Daini Aoitori Gakuen, Okazaki, Japan

[3]Division of Neonatology, Center for Maternal-Neonatal Care, Nagoya University Hospital, Nagoya, Japan

[4]Department of Pediatrics, Nagoya University Graduate School of Medicine, Nagoya, Japan

Manuscript Received: 11 May 2013; Manuscript Accepted: 1 November 2013

Osteopathia striata with cranial sclerosis (OSCS) is an X-linked dominant sclerosing bone dysplasia. Typically affected females show macrocephaly, characteristic facial appearance, cleft palate, mild learning difficulties, hearing loss, sclerosis of the long bones and skull, and longitudinal striations visible on radiographs of the long bones, pelvis and scapulae. Typically affected males usually die at the fetal or early neonatal stage. Because of its variable expressivity, which ranges from asymptomatic to fetal death, clinical diagnosis of OSCS can be difficult. Here, we identify a unique female patient presenting with severe macrocephaly, characteristic facial appearance, developmental delay, and hepatoblastoma. Exome sequencing identified a novel de novo nonsense mutation (c.1045C>T, p.Glu349*) in the *WTX* gene associated with OSCS. The OSCS diagnosis was confirmed in this patient based on the hallmark appearance of longitudinal striations in long bones when viewed by X-ray. *WTX* is also known as a tumor suppressor gene, and somatic mutations in that gene have been identified in Wilms tumors. In addition to this patient, although two patients with OSCS have been reported to have colorectal cancer or ovarian cancer, Wilms tumor has never been reported in association with this disorder. Tumor susceptibility in patients with OSCS is discussed.

Key words: hepatoblastoma; macrocephaly; osteopathia striata with cranial sclerosis; *WTX* mutation

How to Cite this Article:
Fujita A, Ochi N, Fujimaki H, Muramatsu H, Takahashi Y, Natsume J, Kojima S, Nakashima M, Tsurusaki Y, Saitsu H, Matsumoto N, Miyake N. 2014. A novel *WTX* mutation in a female patient with osteopathia striata with cranial sclerosis and hepatoblastoma.
Am J Med Genet Part A 9999:1–5.

INTRODUCTION

Osteopathia striata with cranial sclerosis (OSCS, OMIM 300373) is a rare X-linked dominant sclerosing skeletal bone dysplasia [Jones and Mulcahy, 1968; Behninger and Rott, 2000]. The prevalence of OSCS was estimated to be <1/100,000 [Berenholz et al., 2002] and at least 100 patients have been reported [Zicari et al., 2012]. The clinical features of OSCS are highly variable, ranging from asymptomatic to neonatal lethal conditions-even within the same family, and differ in males and females [Perdu et al., 2010b; Holman et al., 2011; Zicari et al., 2012]. Usually, affected females show macrocephaly with frontal bossing, characteristic facial appearance (widely spaced eyes, epicanthal folds,

Conflict of interest: none.
Grant sponsor: Ministry of Health, Labor Welfare; Grant sponsor: Japan Science Technology Agency; Grant sponsor: Strategic Research Program for Brain Sciences; Grant sponsor: Scientific Research on Innovative Areas-(Transcription cycle)-from the Ministry of Education, Culture, Sports, Science and Technology of Japan; Grant sponsor: Scientific Research from the Japan Society for the Promotion of Science; Grant sponsor: Takeda Science Foundation; Grant sponsor: Hayashi Memorial Foundation for Female Natural Scientists.
*Correspondence to:
Noriko Miyake, M.D., Ph.D. and Naomichi Matsumoto, M.D., Ph.D., Department of Human Genetics, Yokohama City University Graduate School of Medicine, Fukuura 3-9, Kanazawa-ku, Yokohama 236-0004, Japan.
E-mail: nmiyake@yokohama-cu.ac.jp (N.M.), naomat@yokohama-cu.ac.jp (N.M.)
Article first published online in Wiley Online Library (wileyonlinelibrary.com): 00 Month 2014
DOI 10.1002/ajmg.a.36369

broad, and depressed nasal bridge), cleft palate, mild learning difficulties, hearing loss, sclerosis of the long bones and skull, and longitudinal striations visible by X-ray in long bones, the pelvis and scapulae [Konig et al., 1996; Behninger and Rott, 2000; Jenkins et al., 2009]. In the majority of affected males OSCS manifests as embryonic or early neonatal stage lethality, while the few surviving males show cardiac, intestinal, and genitourinary malformations, and hyperostosis [Jenkins et al., 2009]. While OSCS is characterized by longitudinal striations of long bones and cranial sclerosis, the clinical diagnosis can be difficult because of its diverse phenotype, given the wide range of ages at diagnosis.

In 2009, germline truncating mutations or deletions in *WTX* (Wilms tumor gene on the X chromosome protein, also called *FAM123B* or *AMER1*, NM_152424.3) were identified as the cause of OSCS [Jenkins et al., 2009]. WTX functions as a tumor suppressor through Wnt/β-catenin signaling by binding β-catenin and promoting its ubiquitination and degradation, which regulates the level of cytoplasmic β-catenin [Logan and Nusse, 2004; Major et al., 2007; Rivera et al., 2007; Fukuzawa et al., 2010]. Thus, loss of WTX function causes increased levels of cytoplasmic β-catenin, which then translocates into the nucleus. Nuclear β-catenin in turn activates Wnt signaling, leading to tumorigenesis [Logan and Nusse, 2004; Major et al., 2007; Clevers and Nusse, 2012]. However, cancer predisposition in OSCS remains unknown.

Here we report on a female patient affected with OSCS with hepatoblastoma and discuss tumor susceptibility in this disorder.

CLINICAL REPORT

The patient is the first child to a nonconsanguineous healthy mother and father, each of whom was 26 at the time of birth. The patient has a healthy younger brother. Polyhydramnios at 24 weeks of gestation prompted karyotype of amniotic fluid cells (550 band level), which was 46,XX. Her birth weight was 3,138 g (+0.3 SD) and length was 49.5 cm (+1.5 SD). Apgar scores were 9 and 10 at 1 and 5 min, respectively. Macrocephaly (her head circumference was 37.5 cm, +3.3 SD) and muscular ventricular septal defect were recognized. Characteristic facial features were also noted including frontal bossing, apparently widely spaced eyes, blepharophimosis, microtia, posteriorly rotated low-set ears with overfolded helix, broad nasal bridge, small nose, cleft palate, and micrognathia. Extremities were normal. Auditory brainstem response was normal. Her developmental milestones were initially normal, holding her head at 4 months and rolling over at 6 months. After that, development was delayed. She was able to sit, walk holding onto furniture and walk alone at 10, 18, and 23 months, respectively. Cleft palate was surgically corrected at 2 years and 1 month of age, but speech delay was observed, which might be due to the relatively late diagnosis of her conductive hearing loss at about 2 years old. At 2 years and 4 months of age, her height was 78.2 cm (−2.9 SD) and weight was 10.7 kg (−0.8 SD). She showed progressive severe macrocephaly (her head circumference was 56.3 cm, +5.1 SD) with frontal bossing, and delayed closure of the anterior fontanelle. She had delayed bone age of carpal bones (equivalent to 6 months old). While she could walk and trot, mild muscle weakness was noticed especially in the lower extremities. At 2 years and 6 months of age, she had mild developmental delay (D.Q. = 60) but no pervasive developmental disorder, since her social interaction and eye-to-eye gaze were intact. She could understand only about 20 words and speak a few words with unclear pronunciation. After speech and occupational therapies were applied, her development was improved. At 5 years, her intelligence quotient was scored as 81 based on the Tanaka-Binet intelligence scale (Japanese version of Stanford–Binet intelligence scale). Now she is 6 years old, and her head circumference is 62.3 cm (+6.8 SD) and height is 103 cm (−2.4 SD). She is able to speak multi-word sentences and communicate without any trouble.

At 2 years and 4 months of age, a plain radiograph of the skull showed increased anteroposterior diameter, mild enlargement of the cranial suture and thickening and sclerosis of skull bones (Fig. 1A). Cranial magnetic resonance imaging showed cerebral ventricular enlargement and hypoplasia of the corpus callosum, but no signs of intracranial hypertension. Abdominal distension was

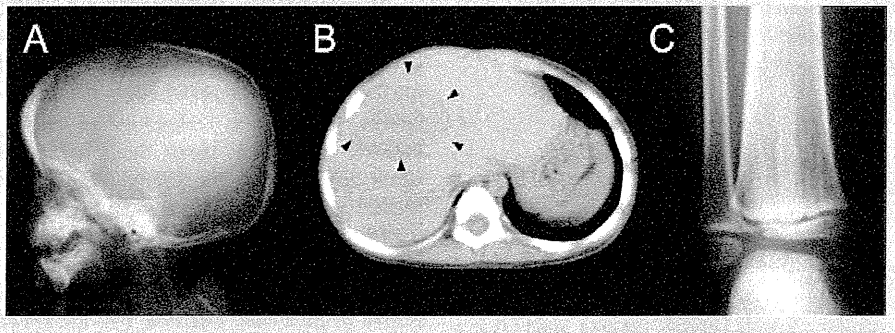

FIG. 1. A: Lateral view of cranial X-ray image of the patient at 2 years and 4 months showed increased anteroposterior diameter, mild enlargement of anterior fontanelle and thickening and sclerosis of skull bones. B: Preoperative computed tomography of liver in the patient. Arrowheads indicate hepatoblastoma (approximately 5 cm in diameter). C: Radiograph of right ankle at 6 years showed longitudinal striations on tibia.

recognized at 2 years and 8 months of age and a large hepatoblastoma spanning was found by computed tomography (Fig. 1B). The preoperative alpha-fetoprotein levels were 557 ng/ml (reference range: <10.0 ng/ml) and tumor stage was PRETEXT II with 84.5% of 5-year survival rate [Meyers et al., 2009]. Her hepatoblastoma was removed by surgery and to date, no evidence of recurrence has been observed.

MATERIALS AND METHODS

Blood samples were collected from the patient, her parents and younger brother after obtaining their written informed consent. DNA was extracted from blood leukocytes and formalin-fixed paraffin-embedded (FFPE) hepatoblastoma tissues containing 80–90% of tumor tissue using QuickGene-610L (Fujifilm, Tokyo, Japan) and QIAamp DNA FFPE Tissue Kit (Qiagen, Hilden, Germany), respectively, according to the manufacturer's instructions. This study was approved by the institutional review board of Yokohama City University School of Medicine.

Exome sequencing was performed on DNA from the patient and her parents. Genome partitioning was performed using the SureSelect Human All Exon v4 kit (51 Mb) (Agilent Technologies, Santa Clara, CA) according to the manufacturer's instructions. Each sample was sequenced by an Illumina HiSeq2000 (Illumina, San Diego, CA) with 101-bp paired-end reads. The reads were aligned to the human reference genome (GRCh37.1/hg19) with Novoalign 2.08.02 (http://www.novocraft.com/). After the removal of PCR duplications by Picard, the variants were called by Genome Analysis Toolkit 1.6–5 (GATK: http://www.broadinstitute.org/gatk/) and annotated by ANNOVAR (2012feb) (http://www.openbioinformatics.org/annovar/) Candidate variants were sequenced with an ABI PRISM 3130xl Genetic Analyzer (Life Technologies Inc., Carlsbad, CA) and analyzed using Sequencher software version 4.10.1 (Gene Codes Corporation, Ann Arbor, MI). Copy number analysis was performed using the CytoScanHD Array (Affymetrix, Santa Clara, CA) according to the manufacturer's protocol. Data were analyzed using Chromosome Analysis Suite software v1.2 .0.225 (Affymetrix). The X-inactivation pattern was investigated using a human androgen receptor (HUMARA) assay, as described [Kondo et al., 2012]. The products were analyzed on an ABI PRISM 3130xl Genetic Analyzer with GeneMapper Software v4.1.1 (Life Technologies Inc.). Two independent experiments were performed.

RESULTS

As the patient was apparently sporadic, we hypothesized her condition was caused by de novo mutation and extracted de novo variants by trio analysis using ES. Furthermore, variants that were registered in dbSNP135, dbSNP137, ESP5400 or our in-house database (exome data of 154 Japanese individuals), variants in segmental duplication and synonymous variants were excluded from the candidates. Only one de novo heterozygous variant, c.1045C>T, which predicts p.Gln349* in the *WTX* gene (NM_152424.3), was left as a pathogenic candidate and confirmed by Sanger sequencing (Fig. 2A).

The SNP array detected no pathogenic copy number variations in the patient and X-inactivation pattern was not skewed in the peripheral blood (39:61). The child shared numerous rare and common variants with her parents, which we conclude confirms biologic parentage. Taken together, we conclude that the novel variant identified here is the causative mutation for this patient's syndrome. In addition, the longitudinal striations on radiographs of the long bones were retrospectively confirmed as one of the representative clinical signs of OSCS (Fig. 1C). Furthermore, Sanger sequencing of c.1045C>T in hepatoblastoma tissue excludes a deletion at least in this genomic position as the peak height of wild type and mutant alleles in the electropherograms was similar in hepatoblastoma tissue like the peripheral blood (Fig. 2B).

DISCUSSION

In this study, a novel nonsense mutation in the *WTX* gene was found in a girl with OSCS and hepatoblastoma. Similar to the previous reports describing *WTX* mutations in OSCS [Zicari et al., 2012], p. Gln349* in the present patient resides at the first APC binding domain of the 5′ region of the WTX protein.

As *WTX* is a tumor suppressor gene, cancer predisposition has been discussed in OSCS. Somatic *WTX* mutations or deletions were detected in 6–30% of Wilms tumor [Fukuzawa et al., 2010]. However, as only two of 64 patients with OSCS and germline mutations or deletions of *WTX* had colorectal cancer or ovarian cancer which developed in adult stage [Jenkins et al., 2009; Perdu et al., 2010a], the cancer predisposition has been suggested as less likely [Jenkins et al., 2009]. Interestingly, unilateral or bilateral Wilms tumors have been found to be associated with nephrogenic rests (known as precursor regions), in 41% and 99% of cases, respectively [Beckwith et al., 1990]. However, approximately only 1% of Wilms tumors develop from nephrogenic rests [Fukuzawa et al., 2010]. It was important to explain the discrepant rates of tumorigenesis in somatic versus germline mutations. It was hypothesized that *WTX* mutations were associated with the late stage of Wilms tumor development and tumorigenesis requires the additional hits on the other loci, like *WT1* or *CTNNB1* [Ruteshouser et al., 2008; Wegert et al., 2009; Fukuzawa et al., 2010].

Hepatoblastoma is a rare tumor with the estimated prevalence of 8.7 and 5.1 cases per million children <1 and 1–4 years, respectively [Howlader et al., 2012]. Significantly, hepatoblastomas have been observed frequently in children affected with familial adenomatous polyposis coli (FAP; OMIM 175100) caused by germline *APC* mutations and Beckwith–Wiedemann syndrome (OMIM 130650), with the relative risk of 847 and 2,280 times higher than general population, respectively [Giardiello et al., 1991; DeBaun and Tucker, 1998; Spector and Birch, 2012]. Like *WTX*, *APC* participates in the degradation of β-catenin, suggesting that germline mutations in each of these genes are associated with tumorigenesis due to the perturbation of Wnt/β-catenin signaling. Further reports of additional patients with OSCS are necessary to address tumor susceptibility in OSCS.

X-inactivation studies in 23 female patients with OSCS and *WTX* abnormalities, including the present patient, have shown random X-inactivation patterns for all patients [Jenkins et al., 2009; Herman et al., 2013; Holman et al., 2013]. As three patients with a severe clinical phenotype showed random X-inactivation [Herman et al., 2013; Jenkins et al., 2009], Herman et al. [2013] suggested that X-inactivation might not correlate with clinical severity. Or,

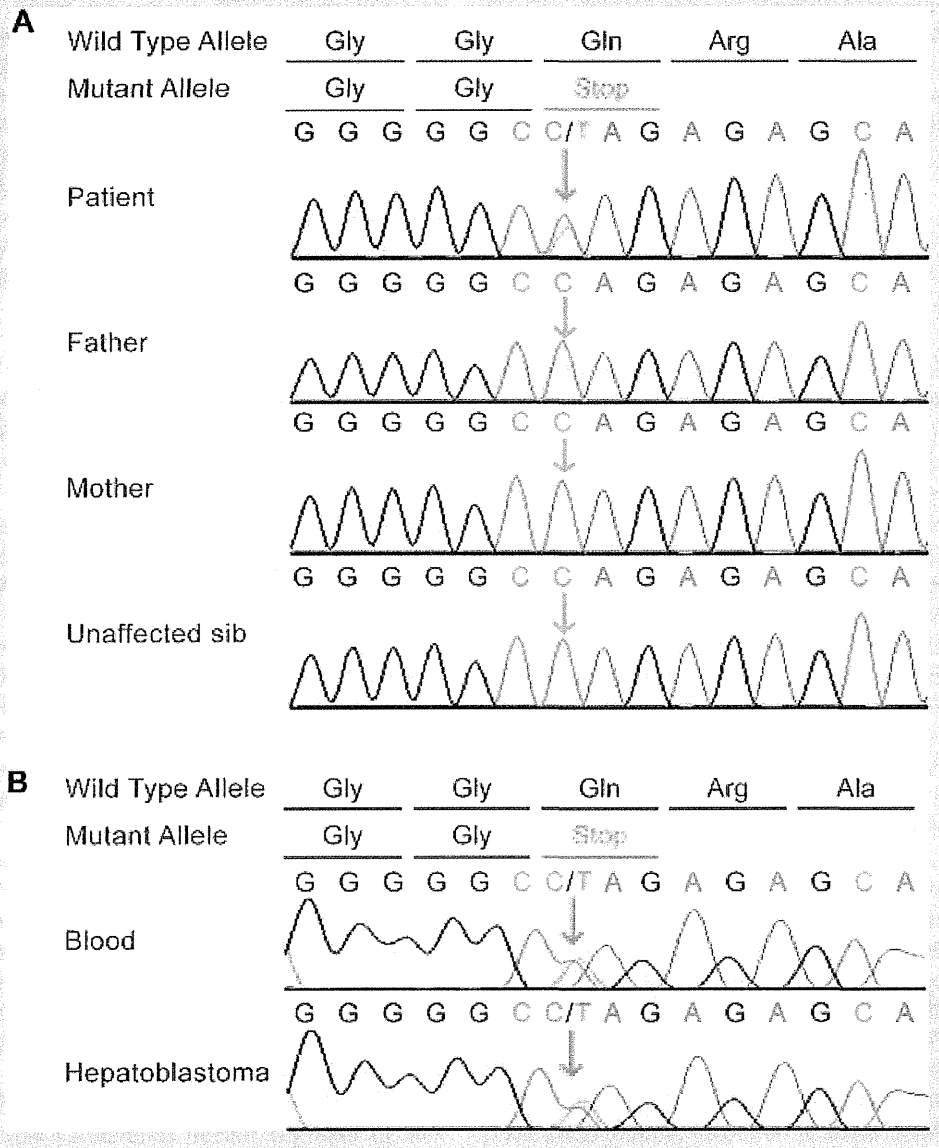

FIG. 2. Electropherogram of a *WTX* mutation, c.1045C>T. A: The heterozygous mutation, c.1045C>T was observed in the patient (red arrow), while no mutation was found in her father, mother and unaffected sib (blue arrow). B: The heterozygous *WTX* mutation in the peripheral blood leukocytes (upper) and hepatoblastoma tissue (lower).

marked skewing leading to a lack of wild-type allele expression might cause lethality similar to affected male patients hemizygous for a null *WTX* allele.

In conclusion, we identified a novel *WTX* mutation (c.1045C>T, p.Gln349*) in a female with OSCS and hepatoblastoma. Tumor susceptibility of germline *WTX* mutations should be considered in the clinical examination of patients with OSCS.

ACKNOWLEDGMENTS

We thank the patient and her family for participating in this study. We also thank Ms. S. Sugimoto and K. Takabe for their technical assistance. This work was supported by research grants from the Ministry of Health, Labor and Welfare (N. Matsumoto, N. Miyake), the Japan Science and Technology Agency (N. Matsumoto), the Strategic Research Program for Brain Sciences (N. Matsumoto) and a Grant-in-Aid for Scientific Research on Innovative Areas-(Transcription cycle)-from the Ministry of Education, Culture, Sports, Science and Technology of Japan (N. Matsumoto), a Grant-in-Aid for Scientific Research from the Japan Society for the Promotion of Science (H. Saitsu, N. Matsumoto, N. Miyake), the Takeda Science Foundation (N. Matsumoto, N. Miyake), and the Hayashi Memorial Foundation for Female Natural Scientists (N. Miyake).

REFERENCES

Beckwith JB, Kiviat NB, Bonadio JF. 1990. Nephrogenic rests, nephroblastomatosis, and the pathogenesis of Wilms' tumor. Pediatr Pathol 10:1–36.

Behninger C, Rott HD. 2000. Osteopathia striata with cranial sclerosis: Literature reappraisal argues for X-linked inheritance. Genet Couns 11:157–167.

Berenholz L, Lippy W, Harrell M. 2002. Conductive hearing loss in osteopathia striata-cranial sclerosis. Otolaryngol Head Neck Surg 127:124–126.

Clevers H, Nusse R. 2012. Wnt/beta-catenin signaling and disease. Cell 149:1192–1205.

DeBaun MR, Tucker MA. 1998. Risk of cancer during the first four years of life in children from the Beckwith–Wiedemann syndrome registry. J Pediatr 132:398–400.

Fukuzawa R, Holman SK, Chow CW, Savarirayan R, Reeve AE, Robertson SP. 2010. WTX mutations can occur both early and late in the pathogenesis of Wilms tumour. J Med Genet 47:791–794.

Giardiello FM, Offerhaus GJ, Krush AJ, Booker SV, Tersmette AC, Mulder JW, Kelley CN, Hamilton SR. 1991. Risk of hepatoblastoma in familial adenomatous polyposis. J Pediatr 119:766–768.

Herman SB, Holman SK, Robertson SP, Davidson L, Taragin B, Samanich J. 2013. Severe osteopathia striata with cranial sclerosis in a female case with whole WTX gene deletion. Am J Med Genet Part A 161A:594–599.

Holman S, Morgan T, Baujat G, Cormier-Daire V, Cho TJ, Lees M, Samanich J, Tapon D, Hove H, Hing A, Hennekam R, Robertson S. 2013. Osteopathia striata congenita with cranial sclerosis and intellectual disability due to contiguous gene deletions involving the WTX locus. Clin Genet 83:251–256.

Holman SK, Daniel P, Jenkins ZA, Herron RL, Morgan T, Savarirayan R, Chow CW, Bohring A, Mosel A, Lacombe D, Steiner B, Schmitt-Mechelke T, Schroter B, Raas-Rothschild A, Minaur SG, Porteous M, Parker M, Quarrell O, Tapon D, Cormier-Daire V, Mansour S, Nash R, Bindoff LA, Fiskerstrand T, Robertson SP. 2011. The male phenotype in osteopathia striata congenita with cranial sclerosis. Am J Med Genet Part A 155A:2397–2408.

Howlader N, Noone A, Krapcho M, Neyman N, Aminou R, Altekruse S, Kosary C, Ruhl J, Tatalovich Z, Cho H, Mariotto A, Eisner M, Lewis D, Chen H, Feuer E, Cronin K. 2012. SEER Cancer Statistics Review, 1975–2009 (Vintage 2009. Populations). National Cancer Institute.

Jenkins ZA, van Kogelenberg M, Morgan T, Jeffs A, Fukuzawa R, Pearl E, Thaller C, Hing AV, Porteous ME, Garcia-Minaur S, Bohring A, Lacombe D, Stewart F, Fiskerstrand T, Bindoff L, Berland S, Ades LC, Tchan M, David A, Wilson LC, Hennekam RC, Donnai D, Mansour S, Cormier-Daire V, Robertson SP. 2009. Germline mutations in WTX cause a sclerosing skeletal dysplasia but do not predispose to tumorigenesis. Nat Genet 41:95–100.

Jones MD, Mulcahy ND. 1968. Osteopathia striata, osteopetrosis, and impaired hearing. A case report. Arch Otolaryngol 87:116–118.

Kondo Y, Saitsu H, Miyamoto T, Nishiyama K, Tsurusaki Y, Doi H, Miyake N, Ryoo NK, Kim JH, Yu YS, Matsumoto N. 2012. A family of oculofaciocardiodental syndrome (OFCD) with a novel BCOR mutation and genomic rearrangements involving NHS. J Hum Genet 57:197–201.

Konig R, Dukiet C, Dorries A, Zabel B, Fuchs S. 1996. Osteopathia striata with cranial sclerosis: Variable expressivity in a four generation pedigree. Am J Med Genet 63:68–73.

Logan CY, Nusse R. 2004. The Wnt signaling pathway in development and disease. Annu Rev Cell Dev Biol 20:781–810.

Major MB, Camp ND, Berndt JD, Yi X, Goldenberg SJ, Hubbert C, Biechele TL, Gingras AC, Zheng N, Maccoss MJ, Angers S, Moon RT. 2007. Wilms tumor suppressor WTX negatively regulates WNT/beta-catenin signaling. Science 316:1043–1046.

Meyers RL, Rowland JR, Krailo M, Chen Z, Katzenstein HM, Malogolowkin MH. 2009. Predictive power of pretreatment prognostic factors in children with hepatoblastoma: A report from the Children's Oncology Group. Pediatr Blood Cancer 53:1016–1022.

Perdu B, de Freitas F, Frints SG, Schouten M, Schrander-Stumpel C, Barbosa M, Pinto-Basto J, Reis-Lima M, de Vernejoul MC, Becker K, Freckmann ML, Keymolen K, Haan E, Savarirayan R, Koenig R, Zabel B, Vanhoenacker FM, Van Hul W. 2010a. Osteopathia striata with cranial sclerosis owing to WTX gene defect. J Bone Miner Res 25: 82–90.

Perdu B, Lakeman P, Mortier G, Koenig R, Lachmeijer A, Van Hul W. 2010b. Two novel WTX mutations underscore the unpredictability of male survival in osteopathia striata with cranial sclerosis. Clin Genet 80:383–388.

Rivera MN, Kim WJ, Wells J, Driscoll DR, Brannigan BW, Han M, Kim JC, Feinberg AP, Gerald WL, Vargas SO, Chin L, Iafrate AJ, Bell DW, Haber DA. 2007. An X chromosome gene, WTX, is commonly inactivated in Wilms tumor. Science 315:642–645.

Ruteshouser EC, Robinson SM, Huff V. 2008. Wilms tumor genetics: Mutations in WT1, WTX, and CTNNB1 account for only about one-third of tumors. Genes Chromosomes Cancer 47:461–470.

Spector LG, Birch J. 2012. The epidemiology of hepatoblastoma. Pediatr Blood Cancer 59:776–779.

Wegert J, Wittmann S, Leuschner I, Geissinger E, Graf N, Gessler M. 2009. WTX inactivation is a frequent, but late event in Wilms tumors without apparent clinical impact. Genes Chromosomes Cancer 48: 1102–1111.

Zicari AM, Tarani L, Perotti D, Papetti L, Nicita F, Liberati N, Spalice A, Salvatori G, Guaraldi F, Duse M. 2012. WTX R353X mutation in a family with osteopathia striata and cranial sclerosis (OS-CS): Case report and literature review of the disease clinical, genetic and radiological features. Ital J Pediatr 38:27.